DOI: 10.1002/ejic.200700586

Transition-Metal Porous Coordination Polymers with a Podand Ligand: Structure of Discrete Water Clusters and Variable-Temperature Magnetism

Subhadip Neogi,[a] E. Carolina Sañudo,[b] and Parimal K. Bharadwaj*[a]

Keywords: Water clusters / Coordination polymers / Metal–organic frameworks / Podand ligands / Magnetism

The podand ligand tris(4-carboxy-2-phenoxyethyl)amine ($ptaH_3$) readily reacts with Co^{II}, Mn^{II} and Ni^{II} salts at room temperature to afford porous coordination polymers, $\{Co(ptaH)\cdot 5H_2O\}_n$ (**1**), $\{[Mn(ptaH)(H_2O)]\cdot 4H_2O\}_n$ (**2**), and $\{[Ni(ptaH)(4H_2O)]\cdot 6H_2O\}_n$, (**3**). Crystallographic studies performed on these systems reveal that their structures are based on infinite chains of interlinked metallacycles. The bridging carboxylate groups extend the open framework structures, with oval-shaped voids. Supramolecularly assembled water clusters of different sizes, whose structures are proportionate with the size and shape of the MOFs, fill these voids. While discrete $(H_2O)_{10}$ clusters are present in **1** and **2**, both $(H_2O)_2$ and $(H_2O)_{16}$ clusters occupy the voids in **3**. Magnetic susceptibility measurements, in the temperature range 2–300 K, on **1** and **2** reveal that the metal centers are antiferromagnetically coupled in each case.

Introduction

Supramolecular association of water molecules in diverse environments has been a subject of considerable current interest.[1–5] This is because the key to test and calibrate theoretical studies in order to understand the properties of bulk water is the precise structural data of hydrogen-bonded small water clusters in diverse environments. The advantage of clusters is the possibility to simply vary the size and to investigate the development of properties of the condensed phase in a step by step manner. Bulk water exhibits a fascinating array of properties, some of which are considered anomalous, and this is due to tremendous fluctuations in H-bonding interactions and rearrangement dynamics among the water molecules in a group. However, this diversity of H-bonding interactions is very crucial in the biological world as it can enforce a delicate balance[6] between several possible conformations of enzymes essential for expressing their functional behavior. In the abiological world, the degree of structuring of the water clusters can influence the structure of metal–organic open frameworks (MOF), where both water–MOF and water–water interactions can be the driving force that affects the overall structure. It follows, therefore, that an understanding of the formation of water clusters is important from the perspective of stabilization and functioning of biomolecules, as well as the structure of MOFs. In addition, they are of relevance in the study[7] of cloud and ice formation, solution chemistry, among others.

MOF structures of paramagnetic metal ions are particularly interesting as these may give rise to a series of novel framework structures with potential applications in the fields of molecular magnetism[8] and materials chemistry.[9] A commonly used strategy in building such extended network structures is to employ bridging ligands that are capable of transmitting magnetic interactions in addition to propagating the network.

We have initiated a research program to synthesize porous coordination polymers with the ultimate goal(s) of having new materials for magnetism, supramolecular storage of guest molecules, and catalysis among other applications. We describe here the formation of three MOFs with Mn^{II}, Co^{II}, and Ni^{II} metal ions and a tripodal ligand,[10] with an aromatic carboxylate group at each terminal. The position of the carboxylate groups in the ligand excludes the formation of a homoleptic metal complex and favors the binding of more than one metal ion, which leads to a carboxylate-bridged MOF structure. This ligand, therefore, allows us to study the magnetic behavior of the MOF formed, as well as the structure of the water clusters present in the voids.

Results and Discussion

The MOFs once isolated are found to be stable in air and insoluble in water or any common organic solvent. All the compounds show strong IR absorption bands between 1350 and 1550 cm^{-1} characteristic[10] of coordinated carboxylate groups.

[a] Department of Chemistry, Indian Institute of Technology, Kanpur 208016, India
[b] Departament de Química Inorgànica, Universitat de Barcelona, Diagonal 647, 08028 Barcelona, Spain
E-mail: pkb@iitk.ac.in
Supporting information for this article is available on the WWW under http://www.eurjic.org or from the author.

The structure of **1** consists of Co^{II} ions, a partially deprotonated $ptaH^{2-}$ ligand, and water molecules. Hexacoordination of the metal is fulfilled by four carboxylate groups from four different ligand units (Scheme 1). Here, two carboxylate groups donate both their O atoms, one carboxylate group donates one O atom (the other O atom is donated to a different Co^{II} ion), while the fourth carboxylate is protonated and donates a single O atom. This leads to a 2D coordination polymer built from metallacycles that extend along the crystallographic *a* axis (Figure 1). The bridging carboxylate group extends the structure in the third dimension. The position of the H atom attached to the carboxylate group could not be located in the difference maps. In this structure, Co–O(carboxylate) bond lengths span the range 2.018(2)–2.179(2) Å and compare well with the distances found in other octahedral Co^{II}–carboxylate structures.[11] Bond angles around the metal do not deviate significantly from the ideal octahedral coordination geometry. The overall structure of **1** is quite similar to the Cd complex reported by us previously.[10c] However, subtle differences remain between the two structures.

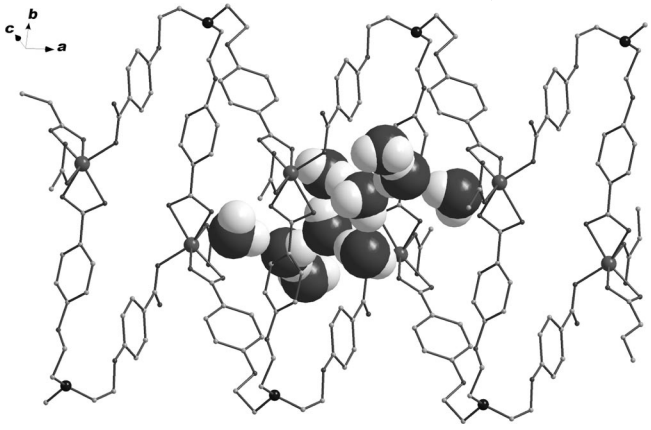

Figure 1. Perspective view of the decameric water cluster in the metallacyclic cavity in **1**.

The coordination mode of Mn^{II} in **2** is slightly different from that of **1**. Each Mn^{II} ion is bonded to four carboxylate groups from four different $ptaH^{2-}$ units and to one water

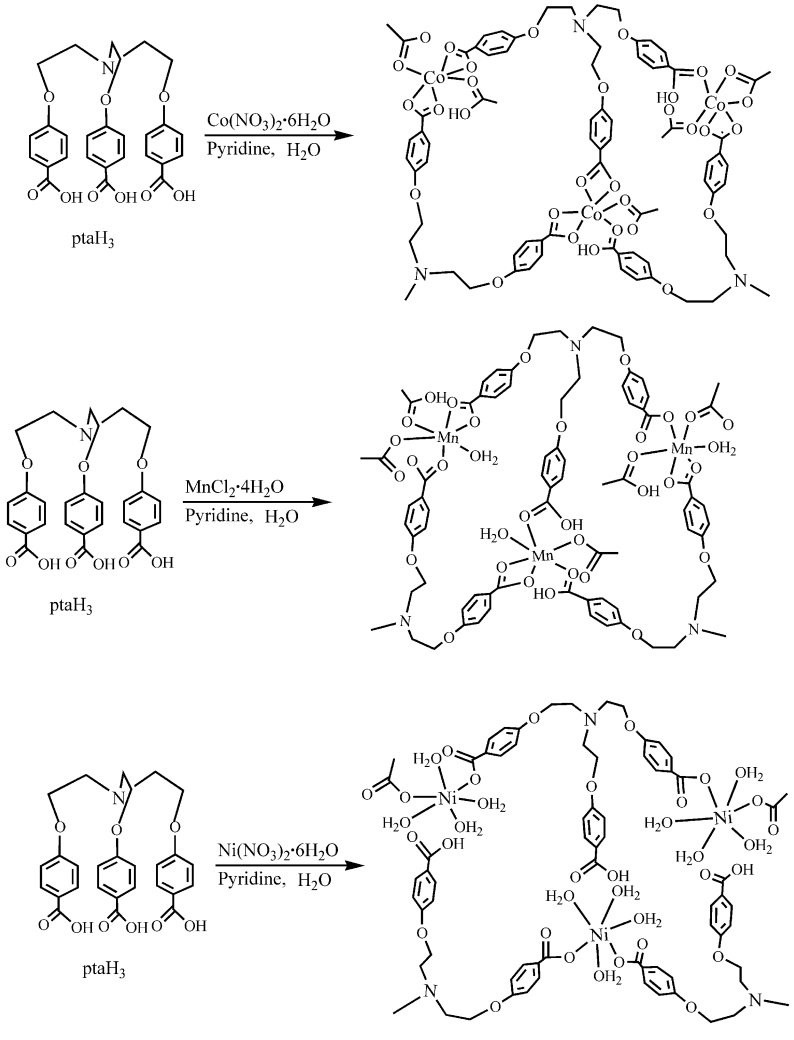

Scheme 1. Bonding scheme for the compounds **1**, **2** and **3**.

molecule. While one carboxylate group donates both its O atoms, the remaining three donate one O atom each, and the sixth coordination position is occupied by an H_2O molecule (Scheme 1). As in **1**, the metallacycles propagate along the crystallographic *a* axis (Figure 2).

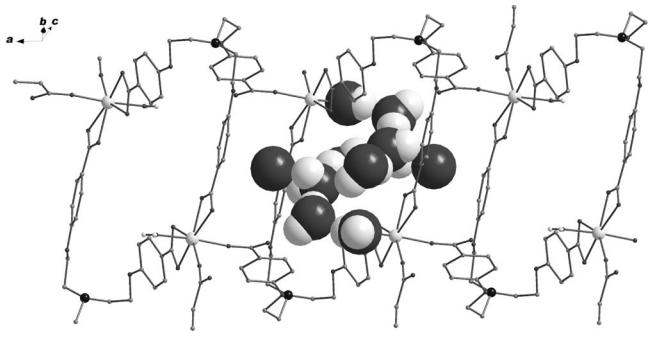

Figure 2. The oval-shaped cavity in **2** with embedded discrete $(H_2O)_{10}$ cluster.

In **3**, only two arms of $ptaH^{2-}$ are bonded to the Ni^{II} ions, while the third arm is free. Each metal ion is hexacoordinate, with ligation from two carboxylate O atoms from two different ligands and four water molecules to form a coordination polymeric chain extending along the crystallographic *a* axis. Two metal-bound water molecules from one polymeric chain is H-bonded to the uncoordinated carboxylate group of another chain to form an overall 2D structure (Figure 3) with cavities that are much larger than those present in **1** and **2**. As in the previous cases, the H atom attached to one of the carboxylate groups of the ligand could not be located in the difference maps.

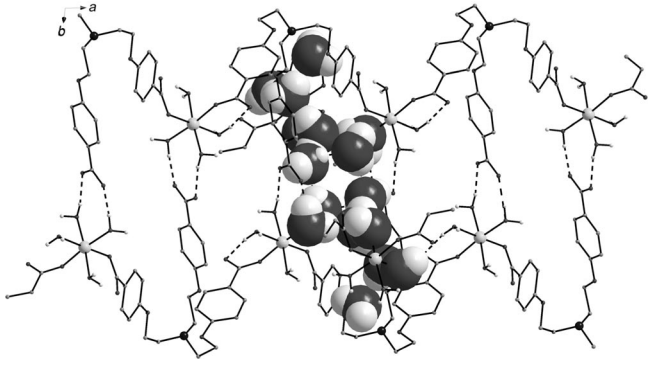

Figure 3. A view of the hexadecameric water cluster inside the H-bonded interlinked metallacycles in **3**. Only the H atoms attached to the water molecules are shown for clarity.

In **1**, the metallacycles have two different dimensions. In the first, two Co^{II} ions exhibit a distance of 9.37 Å, while the distance between two bridgehead nitrogen atoms is 18.92 Å. For the adjacent matallacycle, these dimensions are 10.71 and 18.38 Å, respectively. Similarly, in **2**, in one metallacycle, the $Mn^{II}\cdots Mn^{II}$ distance is 9.98 Å, while the N···N distance is 18.67 Å. For the adjacent metallacycle, these distances are 11.15 and 17.81 Å, respectively. It follows, therefore, that the cavity in **1** is narrower than that of **2**. This difference is reflected in the structures of the $(H_2O)_{10}$ clusters present in the cavities of the two MOFs.

The $(H_2O)_{10}$ cluster in **1** can be viewed as that derived from a cyclic tetramer connected by acyclic trimers at the two opposite ends (Figure 4a). The tetrameric unit is quasiplanar, similar to that predicted theoretically[12] and found in several crystal hydrates.[13] The Ow···Ow distances (2.84–2.76 Å) and O···H–O angles (158.5–169.1°) suggest strong H-bonding interactions between the water molecules. The atoms Ow1, Ow2, Ow1′ and Ow2′ act as H-bond donors to the available carboxylate O atoms with Ow···O (carboxylate) distances in the range 2.76–2.82 Å (Table 1), which maintain strong water–MOF interactions as well. The distance between Ow5 and Ow5′ is within H-bonding distance (2.79 Å). However, these atoms are related by a center of symmetry, and their corresponding H atoms are oriented either towards or away from each other and are not considered to be H-bonded. The H···H separation of 1.07 Å is, however, shorter than the shortest intermolecular H···H separation (1.949 Å) found in the polymorph A of 1,2,3,5-

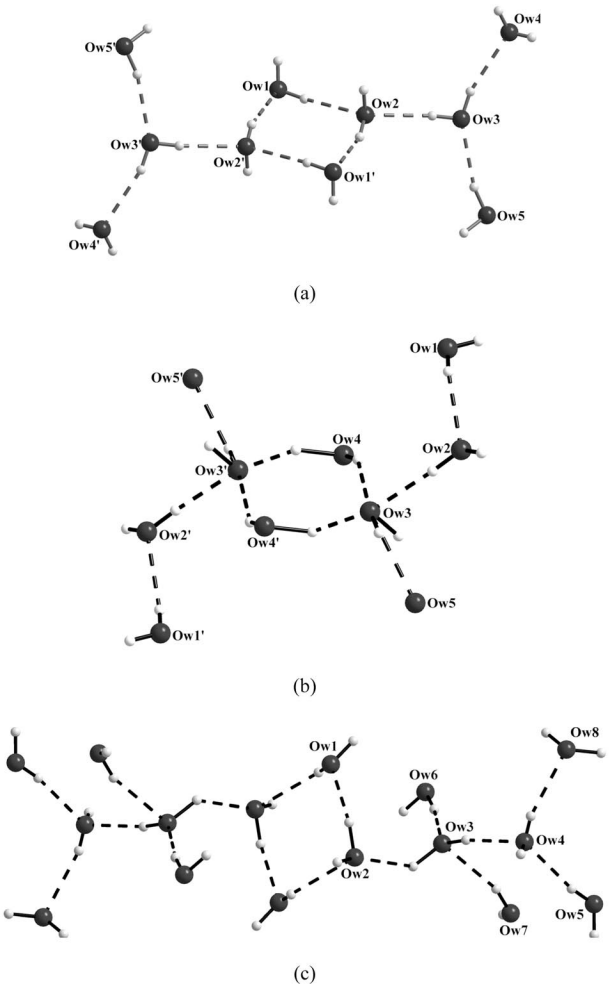

Figure 4. Closer views of the water clusters in (a) **1**, (b) **2**, and (c) **3**, showing the atom numbering scheme.

tetra-*O*-acetyl-β-D-ribofuranose[14a] or in a Zn^{II} complex[14b] that crystallizes in presence of nitrobenzene as the guest. The repulsive interaction associated with this short distance is compensated by strong nonbonding water–MOF interactions.

Table 1. Non-bonding distances [Å] and angles [°] for the water clusters in **1**–**3**.

1			
Ow1···Ow2	2.84(4)	Ow3···Ow5	2.78(3)
Ow1···Ow2′	2.76(4)	Ow1···O9	2.76(3)
Ow2···Ow3	2.79(4)	Ow2···O2	2.82(4)
Ow3···Ow4	2.77(3)	Ow4···O8	2.93(4)
Ow1···Ow2···Ow1′	101.4(9)	Ow2–H···Ow1′	161.9(1)
Ow1···Ow2···Ow3	119.3(9)	Ow3–H···Ow2	169.1(2)
Ow1′···Ow2···Ow3	136.2(9)	Ow3–H···Ow4	158.5(2)
Ow2···Ow3···Ow4	115.2(9)	Ow5–H···Ow3	165.5(6)
Ow2···Ow3···Ow5	107.7(8)	Ow1–H···O9	160.6(3)
Ow4···Ow3···Ow5	135.8(9)	Ow2–H···O2	160.6(2)
Ow1–H···Ow2	168.4(2)	Ow4–H···O8	152.3(2)
2			
Ow1···Ow2	2.75(8)	Ow1···O9	2.75(9)
Ow2···Ow3	2.73(2)	Ow2···O9	2.73(7)
Ow3···Ow4	2.62(3)		
Ow3···Ow4′	2.88(3)		
Ow3···Ow5	2.56(5)		
Ow1···Ow2···Ow3	110.1(5)	Ow2–H···Ow3	171.0(5)
Ow2···Ow3···Ow4	92.6(6)	Ow4–H···Ow3	143.3(8)
Ow2···Ow3···Ow4′	153.7(7)	Ow4′–H···Ow3	136.9(7)
Ow2···Ow3···Ow5	95.9(1)	Ow3–H···Ow5	125.4(2)
Ow4···Ow3···Ow4′	76.9(5)	Ow1–H···O9	168.9(4)
Ow1–H···Ow2	156.3(4)	Ow2–H···O9	162.4(1)
3			
Ow1···Ow2	2.76(9)	Ow1···O8	2.76(7)
Ow1···Ow2′	2.73(7)	Ow2···O5	2.82(9)
Ow2···Ow3	2.82(6)	Ow4···O3	2.67(7)
Ow3···Ow4	2.71(1)	Ow5···O9	2.82(8)
Ow3···Ow6	2.78(6)	Ow6···O6	2.67(8)
Ow3···Ow7	2.96(9)	Ow7···O9	2.57(8)
Ow4···Ow5	2.71(8)	Ow8···O3	2.72(8)
Ow4···Ow8	2.72(9)	Ow9···O5	2.75(6)
Ow9···Ow10	2.72(5)	Ow10···O5	2.80(6)
Ow1···Ow2.Ow1′	92.8(2)	Ow1–H···Ow2′	148.5(2)
Ow2···Ow1···Ow2′	87.2(1)	Ow3–H···Ow2	134.7(2)
Ow2···Ow3···Ow4	111.9(2)	Ow8–H···Ow4	169.3(2)
Ow2···Ow3···Ow6	112.8(2)	Ow9–H···Ow10	169.7(3)
Ow2···Ow3···Ow7	133.5(2)	Ow3–H···Ow4	158.07(2)
Ow3vOw4···Ow5	110.8(1)	Ow4–H···Ow5	159.6(2)
Ow3···Ow4···Ow8	108.5(2)	Ow6–H···Ow3	171.3(2)
Ow1–H···Ow2	147.6(3)	Ow7–H···Ow3	162.7(2)
Ow1–H···O8	156.7(2)	Ow7–H···O9	163.5(2)
Ow2–H···O5	168.6(2)	Ow8–H···O3	162.2(2)
Ow4–H···O3	170.0(3)	Ow9–H···O5	161.6(2)
Ow5–H···O9	175.9(2)	Ow10–H···O5	159.2(2)
Ow6–H···O6	172.4(2)		

The water decamer in **2** has a different structure. The cyclic tetramer is connected to two dimers at opposite ends, where two single water molecules are also H-bonded (Figure 4b). This cluster of water molecules requires more space than those present in **1** and therefore **2** has a larger void space. The water molecules are quite strongly H-bonded to each other as evident from the O···O distances (2.54–2.87 Å) and O···H–O angles (136.9- 171.0°). It is to be noted here that the H atoms attached to Ow5 could not be located in the difference maps. As in the case of **1**, Ow5 and Ow5′ are within H-bonding distance (2.43 Å). Since they are related by a center of symmetry, they are not considered to be H-bonded following the same argument as that made for **1**. This cluster is H-bonded to available carboxylate O atoms with Ow···O distances in the range 2.73–2.75 Å. Buck et al. had suggested[15] that the minimum energy conformation for the decamer is an octameric cube with two water molecules fused at one of the edges, while a more recent calculation showed that two fused parallel pentamers to be the energetically most stable from.[16] Whereas few water decamers[17] with different structures have been identified in metal–ligand hybrids or purely organic crystals, decamers in the form of two fused parallel cyclic pentamers with staggered conformation have been characterized[18] in organic hosts. The structures of the $(H_2O)_{10}$ clusters in **1** and **2** are different from any of these and result from strong water–MOF and water–water interactions.

The large H-bonded cavity in **3** can accommodate higher nuclearity clusters. Eight water molecules from each asymmetric unit are supramolecularly connected to centrosymmetrically related eight more molecules to form a $(H_2O)_{16}$ cluster that occupies the void between two polymeric chains (Figure 3). The structure can be described as a tetrameric core to which two hexameric units are attached at opposite ends. A $(H_2O)_{16}$ cluster in a Cu^{II}-containing MOF was identified earlier[19] to resemble the shape and size of the void for optimum MOF–water interactions. Theoretical calculations on the $(H_2O)_{16}$ cluster[20] show a number of local minima, including fused cubes derived from the D_{2d} and S_4 forms of the $(H_2O)_8$ unit as well as five-membered rings, two of which also contain one six-membered ring. A closer view of the $(H_2O)_{16}$ cluster in **3** (Figure 4c) shows a wide variation in the O···O nonbonding distances (2.96–2.71 Å) relative to 2.759 Å in ice I_h or 2.85 Å in liquid water.[21] The O···O···O angles also vary widely (133.5–87.2°) with an average value of 110.3°. The shape of the cavity in **3** closely follows the shape of the water cluster to maximize the strength as well as the number of interactions with the MOF.

Thermal gravimetric analysis of compound **1** in air shows that weight loss begins at 60 °C, and the loss of 13.6%, which corresponds to the loss of all water molecules (calculated 13.72%), takes place above 200 °C, and soon after, the compound decomposes. The thermogravimetric curve of **2** shows a plateau, and weight loss begins at 60 °C, and the loss of 13.7%, which corresponds to the loss of all water molecules (calculated 13.80%), takes place beyond 200 °C. Complete breakdown of the structure takes place at about 270 °C. Thermal gravimetric analysis of **3** in air shows that the removal of water occurs in stages, beginning at 50 °C, and the loss of 24%, which corresponds to the loss of all water molecules (calculated 24.1%), takes place above 150 °C. Complete decomposition is achieved above approximately 240 °C.

Magnetic Studies

Since paramagnetic transition metal ions are present with carboxylate bridges in both **1** and **2**, magnetic susceptibility studies were performed on **1** and **2**. Variable-temperature magnetic susceptibility data were collected for **1** in the temperature range 2–300 K with an applied magnetic field of 0.5 T. The susceptibility increases smoothly with decreasing temperature (Figure 5a), and the change in susceptibility as a function of temperature follows the Curie–Weiss law at temperatures above 200 K. The value of the Curie constant (3.38 $cm^3 K mol^{-1}$) is consistent with hexacoordinate high-spin Co^{II} ions (2.8–3.4 $cm^3 K mol^{-1}$) [22]; the Curie–Weiss constant has a negative value of –23.71 K, which indicates antiferromagnetic interactions between the metal centers. When analyzing the χT versus T plot, the decrease observed is due to the depopulation of the J = 5/2 state and the preferential population of the J = 1/2 state, in addition to any possible interaction between the Co^{II} ions. The χT value of 3.14 $cm^3 K mol^{-1}$ per Co^{II} ion at 300 K is in agreement with the expected value for a distorted octahedral Co^{II} ion with strong spin-orbit coupling. As the temperature decreases, so does the value for χT, until at 2 K, it reaches the value of 1.26 $cm^3 K mol^{-1}$ per Co^{II} ion. This value is significantly smaller than that expected for isolated Co^{II} centers (1.875 $cm^3 K mol^{-1}$). The magnetization versus field plot (Figure 5b) saturates at a value of 2.06 at 5.0 T, as expected, which is significantly lower than that predicted by the Brillouin law (Co^{II} ion with spin-orbit coupling S_{eff} = 1/2 and g = 4.33[21]); this further supports a weak antiferromagnetic coupling between the Co^{II} ions in **1**. In the 3D network, the Co^{II} ions are grouped in pairs, bridged by two *syn*-, *anti*-carboxylate arms of the $ptaH^{2-}$ ligands. This type of bonding leads to weak antiferromagnetic interactions,[23] as observed in **1**.

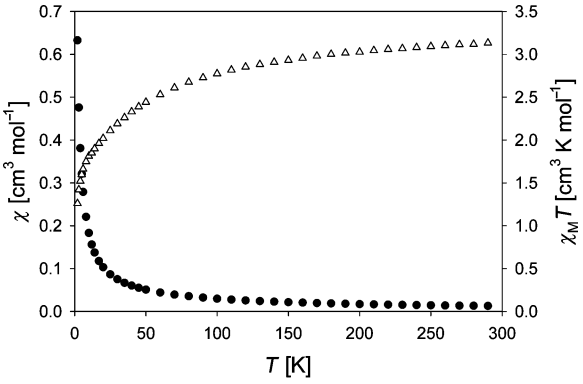

(a)

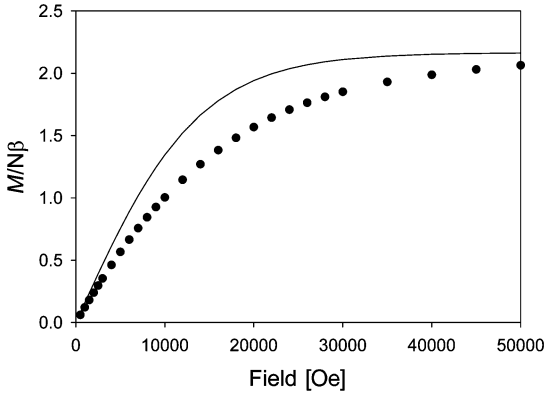

(b)

Figure 5. (a) Temperature dependence of the magnetic susceptibility of **1**. χ is shown as circles, χT is shown as triangles. (b) Magnetization plot for compound **1**. The solid line is the Brillouin function for a Co^{II} ion with spin-orbit coupling.

Figure 6 shows the temperature dependence of the magnetic susceptibility of compound **2** at an applied DC field of 0.3 T in the temperature range 2–300 K and at 200 G below 25 K. In the solid-state structure of **2**, the Mn^{II} ions are arranged in dimers, which, in turn, are organized into a 3D network by the ligands. The dimers are held at an average distance of 10 Å by the $ptaH^{2-}$ ligand, and thus, from a magnetic point of view, the sample has been treated as isolated $[Mn^{II}]_2$ units. The χT product at 300 K has a value of 9.2 $cm^3 K mol^{-1}$, slightly above that expected for two noninteracting Mn^{II} ions (4.375 $cm^3 K mol^{-1}$ per Mn^{II}, S = 5/2). As the temperature decreases, the χT product decreases very slowly to a value of 8.0 $cm^3 K mol^{-1}$ at 50 K and then sharply decreases to 1.1 $cm^3 K mol^{-1}$ at 2 K, which indicates weak antiferromagnetic coupling between the manganese centers, leading to S = 0. The magnetization at 2 K rises continuously with the field to a value of 2.8 at 5 T, without reaching saturation, and confirms the S = 0 value predicted from the susceptibility versus T data. A simple Van Vleck equation[24] for a dimeric S = 5/2 system was used to fit the experimental data. A good agreement between the experimental and calculated data was obtained for J = –0.70 cm^{-1} and g = 2.07, with a TIP of 120×10^{-6} $cm^3 mol^{-1}$ over the entire temperature range. The fit is shown in Figure 5 as a solid line. The weakness of the coupling is easily explained, given the very long Mn–Mn separation: the only possible exchange pathways are two *syn*-, *anti*-carboxylate groups from the ligand unit that hold the Mn^{II} ions 3.86 Å apart. Only very weak coupling can be expected under these conditions, as confirmed by the experimental data. We have recorded FTIR spectra of all three compounds (see Supporting Information) to characterize the vibrational stretching frequency of the O–H bond of the water clusters. In each case, a broad peak appears that centers around 3420 cm^{-1}, which can be attributed to the water cluster. The IR spectrum of ice[13] shows the O–H stretching band at 3220 cm^{-1}, while this stretching vibration in liquid water[13] appears at 3490 and 3280 cm^{-1}. This suggests that the water clusters in **1**–**3** show O–H stretching vibrations similar to that of liquid water. This broad band significantly reduces on heating the compounds under vacuum (0.1 mm), which suggests that the water molecules escape from the lattice. Deliberate exposure to water vapor does not lead to reabsorption of water into the

lattice as monitored by FTIR spectroscopy. Powder X-ray diffraction patterns of the compounds before and after desolvation show major changes in the peak positions as well as in their intensities. Therefore, loss of water from the lattice leads to the breakdown of the framework structure, which supports the thermal analysis results.

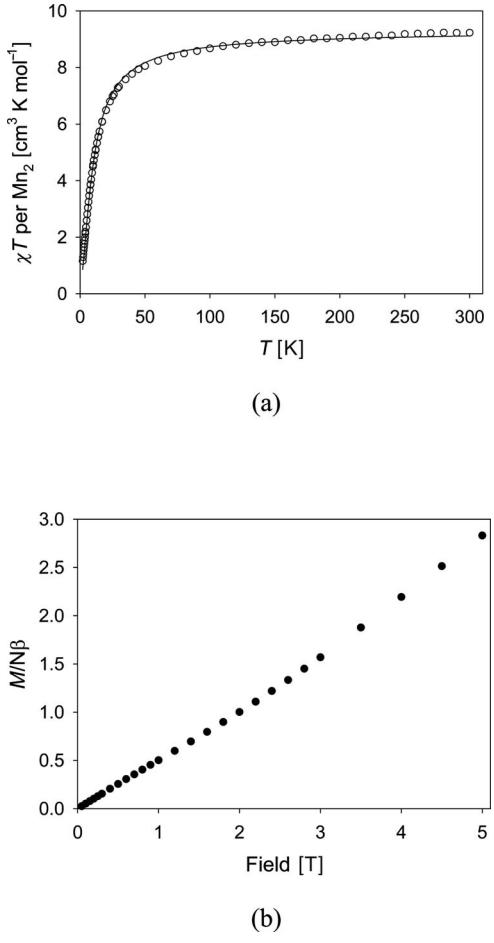

Figure 6. (a) Temperature dependence of the magnetic susceptibility of **2**. (b) Magnetization versus field plot at 2 K for compound **2**.

Conclusions

In conclusion, we have characterized three different MOF structures of transition-metal ions with the tripodal ligand. The large voids present in the MOFs contain supramolecularly bound water molecules of different nuclearity. The size and shape of these water clusters closely follow the available volume of the void spaces. These water clusters act as a "glue" to reinforce the coordination polymeric chains and to extend the open framework structures. Variable-temperature magnetic susceptibility measurements on **1** and **2** reveal that the metal centers are *anti*-ferromagnetically coupled.

Experimental Section

Materials: The metal salts were obtained from Aldrich and used as received. All other chemicals were procured from S. D. Fine Chemicals, India. All solvents were purified prior to use.

Physical Measurements: Spectroscopic data were collected as follows: IR (KBr disk, 400–4000 cm^{-1}) Perkin–Elmer Model 1320; X-ray powder pattern (Cu-K_α radiation at a scan rate of 3°/min, 293 K) Siefert ISODEBYEFLEX-2002 X-ray generator; thermogravimetric analysis (heating rate of 5 °C/min) Perkin–Elmer Pyris 6. Microanalyses for the compounds were obtained from the Central Drug Research Institute, Lucknow, India. Magnetic data were collected at the Unitat de Mesures Magnètiques at the Universitat de Barcelona by using crushed crystals of the sample on a Quantum Design MPMS-XL SQUID magnetometer equipped with a 5 T magnet. Diamagnetic corrections were calculated using Pascal's constants, and an experimental correction for the sample holder was applied.

Synthesis

The ligand tris(4-carboxy-2-phenoxyethyl)amine ($ptaH_3$) was prepared following the method described previously.[10c]

{[Co(ptaH)]·5H$_2$O}$_n$ (1): The tripodal ligand $ptaH_3$ (0.13 g, 0.25 mmol) was dissolved in a thf solution (10 mL) containing tetraethyl ammonium hydroxide (1.2 mL). To this, an aqueous solution of $Co(NO_3)_2{\cdot}6H_2O$ (0.15 g, 0.51 mmol) was added dropwise, and the reaction mixture stirred for 2 h at room temperature. Rectangular pink crystals suitable for X ray diffraction were obtained after 7 d on slow evaporation of the filtrate. Yield approximately 60%. $C_{27}H_{35}CoNO_{14}$: calcd. C 49.39, H 5.37, N 2.13; found C 49.97, H 5.16, N 2.34.

{[Mn(ptaH)(H$_2$O)]·4H$_2$O}$_n$ (2): The tripodal ligand $ptaH_3$ (0.13 g, 0.25 mmol) was dissolved in thf (10 mL) containing tetraethyl ammonium hydroxide solution (1.2 mL) whilst continuously stirring at room temperature. To this, an aqueous solution of $MnCl_2{\cdot}4H_2O$ (0.10 g, 0.50 mmol) was added, and the reaction mixture stirred for 2 h at room temperature. The resulting clear solution was allowed to evaporate at room temperature. Colorless, parallelepiped crystals of **2** were recovered after 10 d. Yield approximately 55%. $C_{27}H_{35}MnNO_{14}$: calcd. C 49.70, H 5.40, N 2.14; found C 50.18, H 5.17, N 2.65.

{[Ni(ptaH)(4H$_2$O)]·6H$_2$O}$_n$ (3): Compound **3** was isolated as dark green rectangular crystals following a similar method to that described for **1**, by using $Ni(NO_3)_2{\cdot}6H_2O$ in place of $Co(NO_3)_3{\cdot}6H_2O$ at room temperature. Yield approximately 60%. $C_{27}H_{45}NNiO_{19}$ (746.36): calcd. C 43.45, H 6.08, N 1.87; found C 43.68, H 6.21, N 2.04.

X-ray Structural Studies: Single-crystal X-ray data on **1**–**3** were collected at 100 K with a Bruker SMART APEX CCD diffractometer by using graphite-monochromated Mo-K_α radiation (λ = 0.71073 Å), and the structures were solved and refined as described earlier.[8a] The H-bonding distances and angles for the water clusters in **1**–**3** are summarized in Table 1, and the crystal and refinement data are collected in Table 2. CCDC-646841 to -646843 for **1**–**3** contain the supplementary crystallographic data for this paper. These data can be obtained free of charge from The Cambridge Crystallographic Data Centre via www.ccdc.cam.ac.uk/data_request/cif.

Supporting Information (see footnote on the first page of this article): IR, TGA, X-ray powder diffraction patterns are presented. Additional figures showing structures of compounds **1**–**3** are also included.

Table 2. Crystal and structure refinement data for **1**–**3**.

Empirical formula	$C_{27}H_{35}NO_{14}Co$ (**1**)	$C_{27}H_{35}NO_{14}Mn$ (**2**)	$C_{27}H_{45}NO_{19}Ni$ (**3**)
Formula weight	656.49	652.50	746.35
Temperature	100(1)K	100(1)K	100(1)K
Radiation, wavelength	Mo-K_α, 0.71073 Å	Mo-K_α, 0.71073 Å	Mo-K_α, 0.71073 Å
Crystal system	triclinic	triclinic	triclinic
Space group	$P\bar{1}$	$P\bar{1}$	$P\bar{1}$
a [Å]	10.2111(9)	10.743(5)	11.203(2)
b [Å]	11.3529(10)	12.614(5)	11.605(2)
c [Å]	12.2940(11)	12.659(5)	13.237(2)
α [°]	93.265(2)	104.354(5)	91.782(5)
β [°]	97.981(2)	114.121(5)	92.255(5)
γ [°]	94.308(2)	94.527(5)	98.886(5)
V [Å^3]	1404.1(2)	1484.9(11)	1697.8(12)
Z	2	2	2
$\rho_{calcd.}$ [Mg/m^3]	1.553	1.459	1.460
μ [mm^{-1}]	0.686	0.515	0.653
$F(000)$	686	682	788
Reflections collected	9243	9741	11411
Independent reflections	6077	5514	6386
Refinement method	Full-matrix least squares on F^2	Full-matrix least squares on F^2	Full-matrix least squares on F^2
GOF	1.143	1.046	1.146
Final R indices [$I > 2\sigma(I)$]	$R1$ = 0.049, $wR2$ = 0.093	$R1$ = 0.079, $wR2$ = 0.116	$R1$ = 0.060, $wR2$ = 0.098
R indices (all data)	$R1$ = 0.058, $wR2$ = 0.109	$R1$ = 0.097, $wR2$ = 0.171	$R1$ = 0.082, $wR2$ = 0.124

Acknowledgments

P. K. B. acknowledges financial support from the Department of Science and Technology, New Delhi, India (grant No.SR/S5/NM-38/2003). S. N. thanks the CSIR, India for a Senior Research Fellowship. E. C. S acknowledges financial support from the Spanish Government (Grant CTQ2006/03949BQU and for a Juan de la Cierva fellowship).

[1] a) M. Mascal, L. Infantes, J. Chisholm, *Angew. Chem. Int. Ed.* **2006**, *45*, 32; b) L. Infantes, J. Chisholm, S. Motherwell, *CrystEngCommun.* **2003**, *5*, 480; c) J. Chisholm, E. Pidcock, J. Streek, L. Infantes, S. Motherwell, F. H. Allen, *CrystEngCommun* **2006**, *1*, 11; d) L. Infantes, L. Fábián, W. D. S. Motherwell, *CrystEngCommun.* **2007**, *1*, 65.

[2] a) A. Michaelides, S. Skoulika, E. G. Bakalbassis, J. Mrozinski, *Cryst. Growth Des.* **2003**, *3*, 487; b) B. Sreenivasulu, J. J. Vittal, *Angew. Chem. Int. Ed.* **2004**, *43*, 5769.

[3] K. Raghuraman, K. K. Katti, L. J. Barbour, N. Pillarsetty, C. L. Barnes, K. V. Katti, *J. Am. Chem. Soc.* **2003**, *125*, 6955.

[4] a) A. Müller, E. Krickemeyer, H. Bögge, M. Schmidtmann, B. Botar, M. O. Talismanova, *Angew. Chem. Int. Ed.* **2003**, *42*, 2085; b) L. E. Cheruzel, M. S. Pometun, M. R. Cecil, M. S. Mashuta, R. J. Wittebort, R. M. Buchanan, *Angew. Chem. Int. Ed.* **2003**, *42*, 5452.

[5] a) B.-Q. Ma, H.-L. Sun, S. Gao, *Angew. Chem. Int. Ed.* **2004**, *43*, 1374; b) A. Nangia, *Water Clusters in Crystal Hydrates*, Encyclopedia of Supramolecular Chemistry, **2007**, p.1.

[6] A. Ben-Naim, *Biophys. Chem.* **2002**,*101*, 309.

[7] K. Koga, H. Tanaka, X. C. Zen, *Nature* **2000**, *408*, 564.

[8] a) O. Kahn, *Molecular Magnetism*, Wiley-VCH, New York, **1993**; b) J. S. Miller, A. J. Epstein, *Angew. Chem. Int. Ed. Engl.* **1994**, *33*, 385; c) M. Ohba, H. Okawa, *Coord. Chem. Rev.* **2000**, *198*, 313; d) A. J. Tasiopoulos, A. Vinslava, W. Wernsdorfer, K. A. Abboud, G. Christou, *Angew. Chem. Int. Ed.* **2004**, *43*, 2117.

[9] a) S. Kitagawa, R. Kitaura, S.-I. Noro, *Angew. Chem. Int. Ed.* **2004**, *43*, 2334;. b) J. L. C. Rowsell, O. M. Yaghi, *Angew. Chem. Int. Ed.* **2005**, *44*, 4670; c) C. J. Kepert, M. J. Rosseinsky, *Chem. Commun.* **1999**, 375; d) M. Dincă, A. Dailly, Y. Liu, C. M. Brown, D. A. Neumann, J. R. Long, *J. Am. Chem. Soc.* **2006**, *128*, 16876; e) G. Férey, C. Mellot-Draznieks, C. Serre, F. Millange, J. Dutour, S. Surblé, I. Margiolaki, *Science* **2005**, *309*, 2040; f) C.-D. Wu, W. Lin, *Angew. Chem. Int. Ed.* **2005**, *44*, 1958.

[10] a) S. Neogi, G. Savitha, P. K. Bharadwaj, *Inorg. Chem.* **2004**, *43*, 3771; b) S. Neogi, P. K. Bharadwaj, *Inorg. Chem.* **2005**, *44*, 816; c) S. Neogi, P. K. Bharadwaj, *Cryst. Growth Des.* **2006**, *6*, 433; d) S. Neogi, P. K. Bharadwaj, *Polyhedron* **2006**, *25*, 1491.

[11] R. H. Groeneman, L. R. MacGillivray, J. L. Atwood, *Inorg. Chem.* **1999**, *38*, 208.

[12] a) S. Pal, N. B. Sankaran, A. Samanta, *Angew. Chem. Int. Ed.* **2003**, *42*, 1741; b) S. Supriya, S. Manikumari, P. Raghavaiah, S. K. Das, *New J. Chem.* **2003**, *27*, 218.

[13] J. D. Cruzan, L. B. Braly, K. Liu, M. G. Brown, J. G. Loeser, R. J. Saykally, *Science* **1996**, *271*, 59.

[14] a) P. Bombicz, M. Czugler, R. Tellgren, A. Kálmán, *Angew. Chem. Int. Ed.* **2003**, *42*, 1957; b) S. Das, P. K. Bharadwaj, *Inorg. Chem.* **2006**, *45*, 5257.

[15] U. Buck, F. Huisken, *Chem. Rev.* **2000**, *100*, 3863.

[16] S. Maheswary, N. Patel, N. Sathyamurthy, A. D. Kulkarni, S. R. Gadre, *J. Phys. Chem. A* **2001**, *105*, 10525.

[17] a) N.-H. Hu, Z.-G. Li, J.-W. Xu, H.-Q. Jia, J.-J. Niu, *Cryst. Growth Des.* **2007**, *7*, 15; b) M. Estrader, J. Ribas, V. Tangoulis, X. Solans, M. F. Bardia, M. Maestro, C. Diaz, *Inorg. Chem.* **2006**, *45*, 8239; c) M. Yoshizawa, T. Kusukawa, M. Kawano, T. Ohhara, I. Tanaka, K. Kurihara, N. Nimura, M. Fujita, *J. Am. Chem. Soc.* **2005**, *127*, 2798; d) R. D. Bergougnant, A. Y. Robin, K. M. Fromm, *Cryst. Growth Des.* **2005**, *5*, 1691; e) L. J. Barbour, G. W. Orr, J. L. Atwood, *Nature* **1998**, *393*, 671.

[18] a) O. Ermer, J. Neudörfl, *Chem. Eur. J.* **2001**, *7*, 4961; b) S. K. Ghosh, P. K. Bharadwaj, *Eur. J. Inorg. Chem.* **2006**, 1341.

[19] S. K. Ghosh, P. K. Bharadwaj, *Inorg. Chem.* **2004**, *43*, 6887.

[20] K. D. Jordan, C. J. Tsai, *J. Phys. Chem.* **1993**, *97*, 5208.

[21] a) D. Eisenberg, W. Kauzmann, *The Structure and Properties of Water, Oxford University Press*, Oxford, **1969**; b) N. H. Fletcher, *The Chemical Physics of Ice*, Cambridge University Press, Cambridge, **1970**.

[22] R. L. Carlin *Magnetochemistry*, Springer-Verlag, Berlin, Heidelberg, **1986**.

[23] J. M. Rueff, N. Masciocchi, P. Rabu, A. Sironi, A. Skoulios, *Eur. J. Inorg. Chem.* **2001**, 2843.

[24] C. J. O'Connor, *Prog. Inorg. Chem* **1982**, *29*, 203.

Received: June 5, 2007
Published Online: October 2, 2007

